AD-A183 696 THE SOLAR WIND-MAGNETOSPHERE-IONOSPHERE CURRENT-VOLTAGE RELATIONSHIP(U) NAVAL RESEARCH LAB WASHINGTON DC J A FEDDER ET AL. 29 JUL 87 NRL-MR-6010 1/1

UNCLASSIFIED F/G 4/1 NL

END
9-87
DTIC

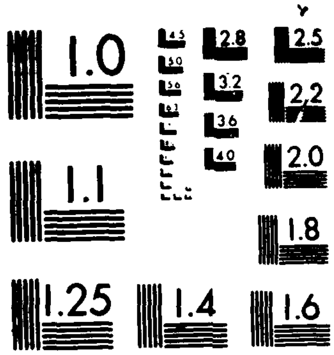

MICROCOPY RESOLUTION TEST CHART
NATIONAL BUREAU OF STANDARDS-1963-A

Naval Research Laboratory

Washington, DC 20375-5000

NRL Memorandum Report 6010

2

The Solar Wind-Magnetosphere-Ionosphere Current-Voltage Relationship

J.A. FEDDER AND J.G. LYON

Geophysical and Plasma Dynamics Branch
Plasma Physics Division

July 29, 1987

SECURITY CLASSIFICATION OF THIS PAGE

REPORT DOCUMENTATION PAGE

1a. REPORT SECURITY CLASSIFICATION UNCLASSIFIED	1b. RESTRICTIVE MARKINGS
2a. SECURITY CLASSIFICATION AUTHORITY 2b. DECLASSIFICATION / DOWNGRADING SCHEDULE	3. DISTRIBUTION / AVAILABILITY OF REPORT Approved for public release; distribution unlimited.
4. PERFORMING ORGANIZATION REPORT NUMBER(S) NRL Memorandum Report 6010	5. MONITORING ORGANIZATION REPORT NUMBER(S)
6a. NAME OF PERFORMING ORGANIZATION Naval Research Laboratory 6b. OFFICE SYMBOL *(If applicable)* Code 4780	7a. NAME OF MONITORING ORGANIZATION
6c. ADDRESS *(City, State, and ZIP Code)* Washington, DC 20375-5000	7b. ADDRESS *(City, State, and ZIP Code)*
8a. NAME OF FUNDING / SPONSORING ORGANIZATION ONR and NASA Office of Naval Research 8b. OFFICE SYMBOL *(If applicable)*	9. PROCUREMENT INSTRUMENT IDENTIFICATION NUMBER
8c. ADDRESS *(City, State, and ZIP Code)* Arlington, VA 22203 Washington, DC 20546 Arlington, VA 22217	10. SOURCE OF FUNDING NUMBERS

PROGRAM ELEMENT NO	PROJECT NO	TASK NO	WORK UNIT ACCESSION NO
W-16/364	61153N	RR033-02-44	DN880-024 DN3[illegible]-[illegible]75

11. TITLE *(Include Security Classification)*
The Solar Wind-Magnetosphere-Ionosphere Current-Voltage Relationship

12. PERSONAL AUTHOR(S)
Fedder, J.A. and Lyon, J.G.

13a. TYPE OF REPORT	13b. TIME COVERED	14. DATE OF REPORT *(Year, Month, Day)*	15. PAGE COUNT
Interim	FROM ____ TO ____	1987 July 29	23

16. SUPPLEMENTARY NOTATION

17. COSATI CODES			18. SUBJECT TERMS *(Continue on reverse if necessary and identify by block number)*
FIELD	GROUP	SUB-GROUP	Magnetohydrodynamics, Birkeland currents, Magnetosphere-Ionosphere Coupling

19. ABSTRACT *(Continue on reverse if necessary and identify by block number)*

The nature of the solar wind-magnetosphere-ionosphere (SW-M-I) coupling has been a subject of intense study and scientific interest. We report results from a numerical simulation of the SW-M-I system which shed light on the physics and behavior of the controlling processes. The current-voltage relationship is characteristic of a magneto-hydrodynamic dynamo with a load operating near short circuit conditions. ~~We discuss~~ the operation of the dynamo, its location with respect to the magnetosphere, and important implications of the results for both the earth and other planets with intrinsic magnetic fields.

20. DISTRIBUTION / AVAILABILITY OF ABSTRACT ☒ UNCLASSIFIED/UNLIMITED ☐ SAME AS RPT. ☐ DTIC USERS	21. ABSTRACT SECURITY CLASSIFICATION UNCLASSIFIED
22a. NAME OF RESPONSIBLE INDIVIDUAL J.D. Huba	22b. TELEPHONE *(Include Area Code)* (202) 767-3630 22c. OFFICE SYMBOL Code 4780

DD FORM 1473, 84 MAR 83 APR edition may be used until exhausted. All other editions are obsolete.

SECURITY CLASSIFICATION OF THIS PAGE

CONTENTS

THE SOLAR WIND-MAGNETOSPHERE-IONOSPHERE
CURRENT-VOLTAGE RELATIONSHIP

I. INTRODUCTION

Magnetospheric convection, electric fields, and Birkeland currents have been an area of intensive research over the past 20 years. Recent reviews with reference to many of the earlier papers include the monograph edited by Potemra [1984] and papers by Hill [1983], Wolf [1983], Burch and Heelis [1980], and Potemra et al. [1980]. The intense interest in this area is motivated largely by a desire to understand the interactions of the SW-M-I system and to be able to predict its effects on near-earth space and man-made systems operating in this region. Impirical studies of the coupling function of the SW-M-I system include Burton et al. [1975], Perreault and Akasofu [1978], and Reiff et al. [1981], which relate the power input to the magnetosphere to solar wind conditions. All these studies indicate that the dynamo power is sensitively controlled by the interplanetary magnetic field, IMF. Stern [1978, 1984] has convincingly argued for a primary dynamo in the magnetopause-magnetosheath region and operating on magnetic field lines open to the solar wind. On the other hand, Heikkila [1984] and others have studied the operation of a dynamo in the magnetospheric boundary layer operating on closed field lines. The results presented here strongly support the Stern model for southward IMF conditions.

A number of previous studies of the high latitude current voltage relationship have been reported. A study by Robinson [1984] using incoherent scatter radar data discovered a linear relationship between the polar cap potential and ionospheric Pedersen currents. Fujii et al. [1981] and Fujii and Iijima [1987] studied the seasonal Birkeland current intensity and discovered that larger currents were coincident with higher ionospheric conductivity. For smaller scale structures, Vickrey et al. [1986], using Dynamics Explorer satellite data, and Lysak [1985], using a theoretical and simulation study, present results which indicate that the magnetosphere dynamo behaves like a current source.

In this paper we report results for the global current-voltage relationship for the SW-M-I system. Since this study is restricted to strong southward IMF, the dynamo which we identify is located on open field lines. We discuss how the dynamo is controlled by ionospheric

Manuscript approved April 8, 1987.

conductivity and in the earth's SW-M-I system operates, under normal conditions, very close to short circuit and at a fraction of the power output which is available. Finally, we discuss the implications of these results for the SW-M-I system: the relationship between open and closed field dynamos, the effect of solar wind conditions, the control of reconnection on the bow, the size of the open field line region, the effects of increased auroral conductivity, and the efficiency of coupling to the solar wind.

II. NUMERICAL MODEL

The simulations are based on the ideal MHD equations which are used to describe the solar wind and the outer (beyond 3.5 R_e) magnetosphere. They are given as follows.

Continuity:

$$\frac{\partial \rho}{\partial t} + \nabla \cdot (\rho \underline{v}) = 0 \tag{1}$$

Momentum balance:

$$\rho \frac{\partial v}{\partial t} + \rho (\underline{v} \cdot \nabla)\underline{v} + \nabla p = \underline{j} \times \underline{B} \tag{2}$$

Energy balance:

$$\frac{\partial \varepsilon}{\partial t} = - \nabla \cdot (\varepsilon + p)\underline{v} + \underline{j} \cdot \underline{E} \tag{3}$$

Faraday's Law:

$$\frac{\partial B}{\partial t} = - \nabla \times \underline{E} \tag{4}$$

Ampere's Law:

$$\mu \underline{j} = \nabla \times \underline{B} \tag{5}$$

Ohm's Law:

$$\underline{E} + \underline{v} \times \underline{B} = 0, \tag{6}$$

where the symbols have their common usage. For the magnetospheric-solar wind region of interest the major error in these equations is the neglect of the so-called Hall term, $m/\rho e(\underline{j} \times \underline{B})$, on the right hand side of (6) [Siscoe, 1982]. These equations are solved as an initial value problem to a quasi steady state for a given solar wind condition.

Our recent simulations have included a number of innovations. First, the development of a fully-nonlinear, high-accuracy algorithm for solution of the MHD equations [Lyon, 1987]. Second, the use of a spider web numerical grid which is rotated around the sun-earth axis to provide a 3-dimensional cylindrical mesh which gives high resolution in important regions (i.e., the dayside magnetopause, the polar open field line region). Third, the inclusion of a model for the conducting ionosphere, which provides a physical inner boundary to the MHD system. Specifically, the ionosphere is modeled electrostatically,

$$\nabla \cdot \underline{\underline{\Sigma}}\, \underline{E} = J_{||}. \tag{7}$$

The parallel current density, $J_{||}$, is calculated at the inner boundary (3.5 R_E geocentric radius) of the MHD mesh. It is mapped along dipole field lines to the ionosphere where the electric field, $\underline{E}$, is computed using a conductivity model for the ionosphere. The electric field is then mapped outward to the inner boundary where it is used as a boundary condition for both the momentum balance equation and for Faraday's Law. The system of equations (1) thru (7) form a closed set with the conductivity, $\underline{\underline{\Sigma}}$, provided. They also constitute a realistic, restricted physical model for magnetosphere-ionosphere coupling. The main effects ignored are the Alfvén propagation time from 3.5 R_e to the ionosphere, the possible existence of field aligned potentials, and the enhancements to conductivity created by precipitating auroral particles.

For the results presented here we have used steady solar wind conditions with density, $n = 5\ cm^{-3}$, velocity, $V = 400$ km sec^{-1}, temperature, $T = 10$ ev, and IMF, $B = 5$ nT southward. We have also used uniform ionospheric conductivities for two reasons: first, the lack of an auroral enhancement model coupled to the MHD; and second, to simplify the interpretation of the results and the identification of dynamo regions, since spatially varying conductivities can lead to polarization and considerable complication of both the current systems and the source dynamos.

III. RESULTS

The results clearly demonstrate the observed morphology of the polar currents and electric fields. Figure 1 is presented as an example showing the polar field aligned currents on the left and the electric potential on the right. Clearly seen are the Region 1 and Region 2 Birkeland current systems on the left as well as the anti-sunward convection over the polar cap and the sunward convection at equatorward latitudes on the right. It is noteworthy that the current densities, total current, electric field, and total potential are all within observed limits, even though the assumed ionospheric conductance of 2.5 mhos is somewhat low for the solar wind conditions. It is also interesting to note the pair of currents flowing opposite to the Region 2 system at the lowest latitudes near 0800 and 1600. These are computational artifacts since the 3.5 R_e inner boundary of the model is not a natural drift surface for ring current plasma. In addition to the currents shown above, the model clearly reproduces the Svalgaard-Mansurov effect [Friis-Christensen, 1984] for East-West IMF conditions, and the NBZ currents [Iijima, 1984] for northward IMF. Superficially at least, the simulation model appears to behave in a manner similar to the SW-M-I system. To further investigate the simulation model and the physical mechanisms operative, it is necessary to adjust available parameters such as the solar wind or the ionosphere.

For this study we adjusted the ionospheric conductivity choosing conductance values of 0.1, 1.25, 2.5 and 5.0 mhos. Figure 2 shows the current-voltage (I-V) relationship (solid line) and the power delivered by the generator (dashed line). The voltage axis marks the total cross polar cap potential while the current axis is the total current in the Region 1 Birkeland current system which flows through the dynamo.

Three features of the I-V curve are striking: the first is the near perfect linearity of the I-V curve, the second is that the physical operating regime of the SW-M-I system is very near the horizontal axis (short circuit current), and the third is that the dynamo does not look like either an intrinsic voltage source (a horizontal line) or an intrinsic current source (a vertical line). The power curve was derived as the product of the current and voltage. It shows an approach to a maximum for an ionospheric conductance below 0.1 mho and also demonstrates that the SW-M-I system is operating at a fraction of the available power because of the high conductance of the ionosphere.

The final result, shown in Fig. 3, is a sketch of the coupling currents, magnetic field, and electric fields for the SW-M-I system projected onto a solar magnetospheric y-z coordinate plane. The Region 1 Birkeland currents toward (away from) the earth on the dawn (dusk) side of the magnetosphere at high latitudes are immediately adjacent to the open-closed field line boundary. As the Region 1 currents reach the magnetopause they bend tailward along the tail-like magnetic field and eventually close perpendicular to the magnetic field through a dynamo region in the polar tail magnetopause-magnetosheath. A small portion of the Region 1 current also closes through a dynamo region in the low latitude boundary layer; however, these currents are in series with the high latitude dynamo which dominates the electromagnetic induction.

The Region 2 currents as they approach the equatorial plane close perpendicular to the magnetic field tailward to the near-earth plasma sheet. Here the electromagnetic forces work as a motor or pump driving the near earth plasma sheet plasma sunward.

IV. DISCUSSION AND CONCLUSIONS

The results described above have allowed us to begin to understand in detail the SW-M-I coupling and dynamo system for southward IMF, how it is controlled by the solar wind, and modifications caused by the ionosphere conductivity. We consider first the I-V diagram (Fig. 2). The I-V curve shown is for a single solar wind condition. As the solar wind conditions change, the curve shifts either to the left or the right without materially changing shape. Increasing (decreasing) either the solar wind velocity or southward IMF causes the curve to shift roughly perpendicular to itself towards the right (left), increasing (decreasing) the power delivered by the dynamo.

The dynamo mechanism can be understood by consideration of the plasma momentum equation (2) [Vasyliunas, 1984]. In the absence of Maxwell stresses applied by a conducting ionosphere and the coupling currents, $\underline{j} \times \underline{B} = 0$; the solar wind flow along the magnetopause and in the nearby magnetosheath is purely hydrodynamic. However, we may consider that two equal and opposite pseudo-currents flow in the plasma; a pressure driven current, $\nabla p \times \underline{B}/B^2$, and a polarization-like current, $\rho/B^2 (\underline{v} \cdot \nabla) \underline{v} \times \underline{B}$. The pressure driven current is directed opposite to the motional electric field, $\underline{E} = - \underline{v} \times \underline{B}$. When a load is added to the system by the ionosphere and the coupling currents, the polarization-like current is reduced and the difference between the pressure driven and the polarization-like currents provides a MHD dynamo mechanism through the Maxwell stresses.

The role of the ionospheric conductivity is to regulate the power delivered by this dynamo through the coupling currents. It does this in two distinct ways. First, it controls the reconnection rate between the IMF and the geomagnetic field on the nose of the magnetosphere by regulating the length of the bow reconnection line, thereby controlling the amount of open magnetic flux in the polar magnetosphere, which has been clearly seen in the results. Second, by regulating the strength of the Region 1 Birkeland currents, it broadens or narrows the "window" [Stern, 1976] in the polar magnetopause for open polar magnetic flux as it passes into the magnetosheath. This narrowing of the window through the magnetopause is clearly seen in Fig. 3 where the sunward and anti-sunward Region 1 Birkeland currents along the polar magnetopause cause a distinct cusp formation in the field lines as they pass through the current sheet. This cusp-like topology for field lines passing through the polar magnetopause is consistent with recent modeling results of Siscoe and Sanchez [1987].

The regulation of the SW-M-I dynamo by the ionospheric conductance on a global scale is very effective. It forces the system to operate near short circuit current on the I-V curve and limits the power extracted from the solar wind to a fraction of that which is available. This behavior is not necessarily the same for other planetary magnetospheres. In particular, for Mercury, where the load is the surface rock conductance of approximately 0.1 mhos, the power conversion should be much more efficient as has been inferred from measurements [Russell et al., 1986].

The results clearly show that the amount of open magnetic flux is controlled by the ionospheric conductivity and the complete SW-M-I coupling system. This strongly implies that, in the simulation model, the magnetic reconnection rate on the nose of the magnetosphere is also controlled by the conductivity and the SW-M-I system and not by any numerical effects. We would suggest that in the magnetosphere a similar control is effective for dayside reconnection, and it is not controlled by resistivity or diffusion or any plasma microphysical effect local to the reconnection region.

The results presented here are consistent with the previous studies of Robinson [1984], Fujii et al. [1981], and Fujii and Iijima [1987]. The Robinson relation between voltage and current corresponding to the left (right) shifts of the I-V curve depending on solar wind conditions, and the Fujii relationship between conductivity and current corresponding to the shifts along the I-V curve caused by conductance changes. The behavior of the dynamo as a current generator at small spatial scales [Vickrey et al., 1986] and at short temporal scales [Lysak, 1985] can be explained by tests we performed using localized enhancements to the polar ionosphere conductance. In these tests the localized enhancements polarized in such a fashion as to keep the ionosphere currents constant; the global coupling of the SW-M-I system remained essentially unaltered.

The results and conclusions presented here apply for solar wind conditions with a strong southward component of the IMF. The limited role of the low latitude boundary layer in dynamo activity clearly may not apply for northward IMF as we have already seen in other simulation results not presented here. However, the state of the SW-M-I system under northward IMF is much more complicated than the relatively straightforward results presented here and requires more analysis.

It is also essential that future work link the auroral conductivity to the magnetospheric dynamics. There exists a strong possibility that the SW-M-I system is self-regulating. That is to say, that an increase in the power from the solar wind can lead to an increase in ionospheric auroral conductivity which in turn reduces the coupling efficiency to the solar wind. The auroral conductivity is also expected to play a strong role in substorm activity through the closure of Region 2 currents in the near earth plasma sheet. Here an increased auroral conductivity can lead to increased Region 2 currents which inject the near earth plasma sheet towards the earth and reduce the northward component of the geomagnetic field near the center of the plasma sheet. This type of behavior suggests an ionospheric substorm trigger for formation of a near earth reconnection region and ring current injection.

Clearly much work remains to be done. We hope to report on the nature of the SW-M-I coupling and dynamo processes for northward IMF in the near future. The link between auroral conductivity and magnetospheric dynamics will require further code development.

ACKNOWLEDGMENTS

This research has been supported by ONR and NASA.

REFERENCES

Burch, J.L. and R.A. Heelis, "IMF Changes and Polar-Cap Electric Fields and Currents," in Dynamics of the Magnetosphere, ed. by Akasofu, S.-I., D. Reidel Publ. Co., Dordrecht, 47, 1980.

Burton, R.K., R.L. McPherron, and C.T. Russell, "The Terrestrial Magnetosphere: A Half-Wave Rectifier of the Interplanetary Electric Field," Science, 189, 717, 1975.

Friis-Christensen, E., "Polar Cap Current Systems," in Magnetoshperic Currents, ed. by T.A. Potemra, Amer. Geophys. U., Washington, DC, 86, 1984.

Fujii, R. and T. Iijima, "The Control of Ionospheric Conductivities on Large Scale Birkeland Current Intensities under Geomagnetic Quiet Conditions," J. Geophys. Res., to be published, 1987.

Fujii, R., T. Iijima, T.A. Potemra, and M. Sugiura, "Seasonal Dependence of Large-Scale Birkeland Currents," Geophys. Res. Lett., 8, 1103, 1981.

Heikkila, Walter J., "Magnetosheric Topology of Fields and Currents," in Magnetospheric Currents, ed. by T.A. Potemra, Amer. Geophys. U., Washington, DC, 208, 1984.

Hill, T.W., "Solar Wind Magnetosphere Coupling," in Solar-Terrestrial Physics, ed. by R.L. Carovillano and J.M. Forbes, D. Reidel Publ. Co., Dordrecht, 261, 1983.

Iijima, Takasi, "Field-Aligned Currents During Northward IMF," in Magnetospheric Currents, ed. by T.A. Potemra, Amer. Geophys. U., Washington, DC 115, 1984.

Lyon, J.G., in preparation, 1987.

Lysak, R.L., "Auroral Electrodynamics with Current and Voltage Generators," J. Geophys. Res., 90, 4178, 1985.

Perreault, P. and S.-I. Akasofu, "A Study of Geomagnetic Storms," Geophys. J.R. Astron. Soc., 54, 547, 1978.

Potemra, Thomas A. ed., Magnetospheric Currents, Amer. Geophys. U., Washington, DC, 1984.

Potemra, T.A., T. Iijima, and N.A. Saflekos, "Large-Scale Characteristics of Birkeland Currents," in Dynamics of the Magnetosphere, ed. by S.-I. Akasofu, D. Reidel Publ. Co., Dordrecht, 165, 1980.

Reiff, P.H., R.W. Spiro, and T.W. Hill, "Dependence of Polar Cap Potential Drop on Interplanetary Parameters," J. Geophys. Res., 86, 7639, 1981.

Robinson, R.M., "K_p Dependence of Auroral Zone Field-Aligned Current Intensity," J. Geophys. Res., 89, 1743, 1984.

Russell, C.T., D.N. Baker, and J.A. Slavin, "The Magnetosphere of Mercury," unpublished manuscript, 1987.

Siscoe, G.L., "Solar System Magnetohydrodynamics," in Solar-Terrestrial Physics, ed. by R.L. Carovillano and J.M. Forbes, D. Reidel Publ. Co., Dordrecht, 11, 1983.

Siscoe, G.L. and E. Sanchez, "An MHD Model for the Complete Open Magnetotail Boundary," submitted to J. Geophys. Res., 1987.

Stern, David P., "A Study of the Electric Field in an Open Magnetospheric Model," J. Geophys. Res., 78, 7292, 1973.

Stern, David P., "Magnetospheric Dynamo Processes," in Magnetospheric Currents, ed. by T.A. Potemra, Amer. Geophys. U., Washington, DC, 200, 1984.

Vasyliunas, Vytenis M., "Fundamentals of Current Description," in Magnetospheric Currents, ed. by T.A. Potemra, Amer. Geophys. U., Washington, DC, 63, 1984.

Vickrey, J.F., R.C. Livingston, N.B. Walker, T.A. Potemra, R.A. Heelis, M.C. Kelley, and F.J. Rich, "On the Current-Voltage Relationship of the Magnetospheric Generator at Intermediate Spatial Scales," Geophys. Rev. Lett., 13, 495, 1986.

Wolf, R.A., "The Quasi-Static (Slow-Flow) Region of the Magnetosphere," in Solar-Terrestrial Physics, ed. by R.L. Carovillano and J.M. Forbes, D. Reidel Publ. Co., Dordrecht, 303, 1983.

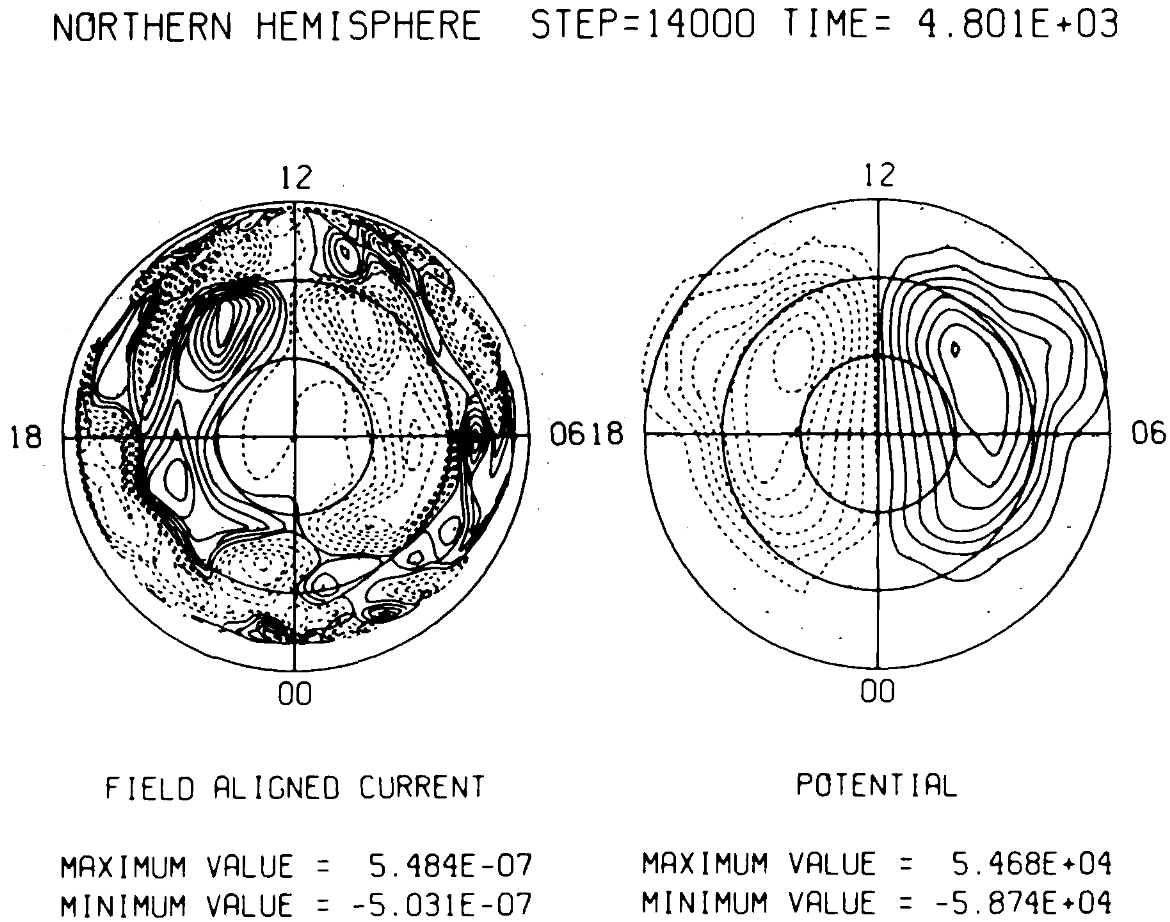

Figure 1. The field-aligned currents (amp m^{-2}) on the left and electric potential (volts) on the right as a function of magnetic latitude, 60°-90°, and solar hour angle. For currents, the solid (dashed) contours indicate out of (into) the ionosphere; and for voltage, solid (dashed) contours indicate positive (negative) potential. The current contours show the Region 1 system between 70° and 80° magnetic latitudes and the Region 2 currents at lower latitude. The potential contours show the anti-sunward plasma convection above about 75° latitude and sunward convection at lower latitudes.

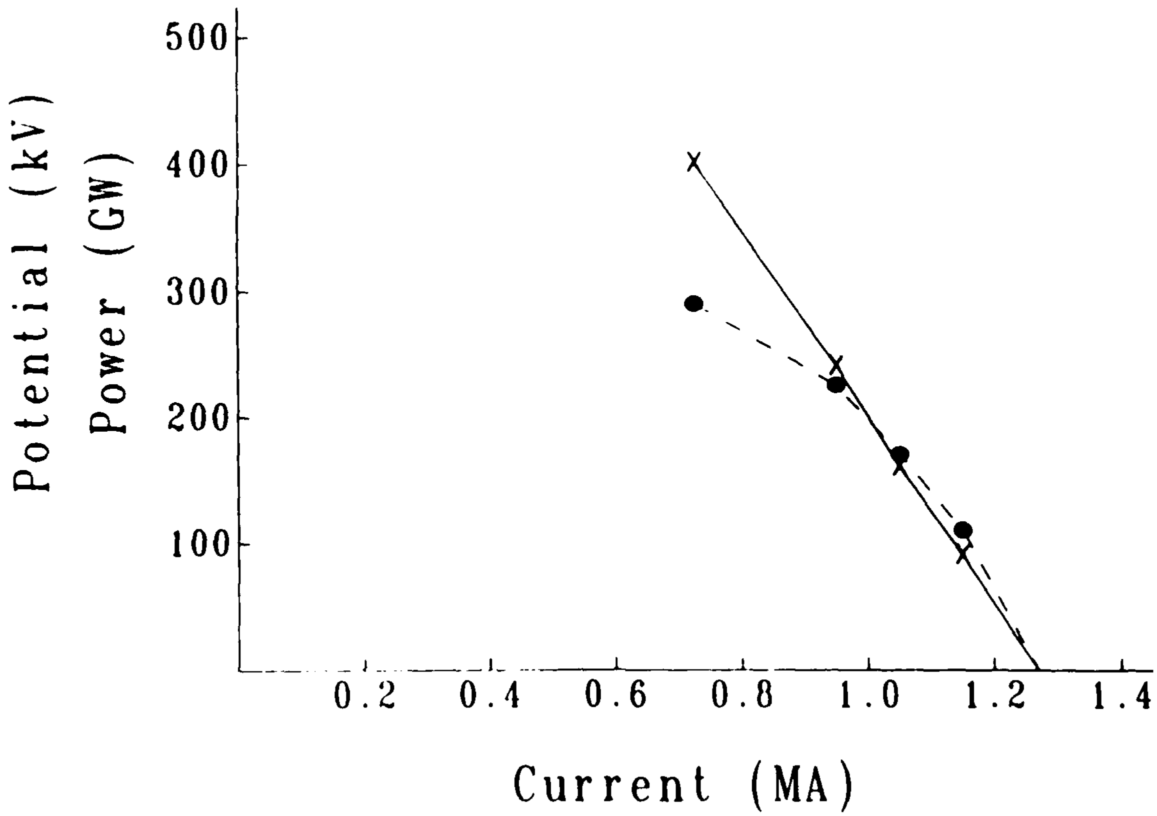

Figure 2. The SW-M-I current-voltage relation (solid curve) and the power relation (dashed curve) for a variable ionospheric conductance. The data points indicated on the curves are for uniform conductances of 0.1, 1.25, 2.5, 5.0 mhos left to right, respectively. Over this range of conductance the I-V curve is almost perfectly linear whereas the power curve approaches a maximum at the lowest conductance. Since the average effective conductance of the polar regions is about 5 mhos and possibly considerably more during active times, the curves indicate that the SW-M-I dynamo operates near short circuit current conditions; and therefore, the system inefficiently converts the power available in the solar wind.

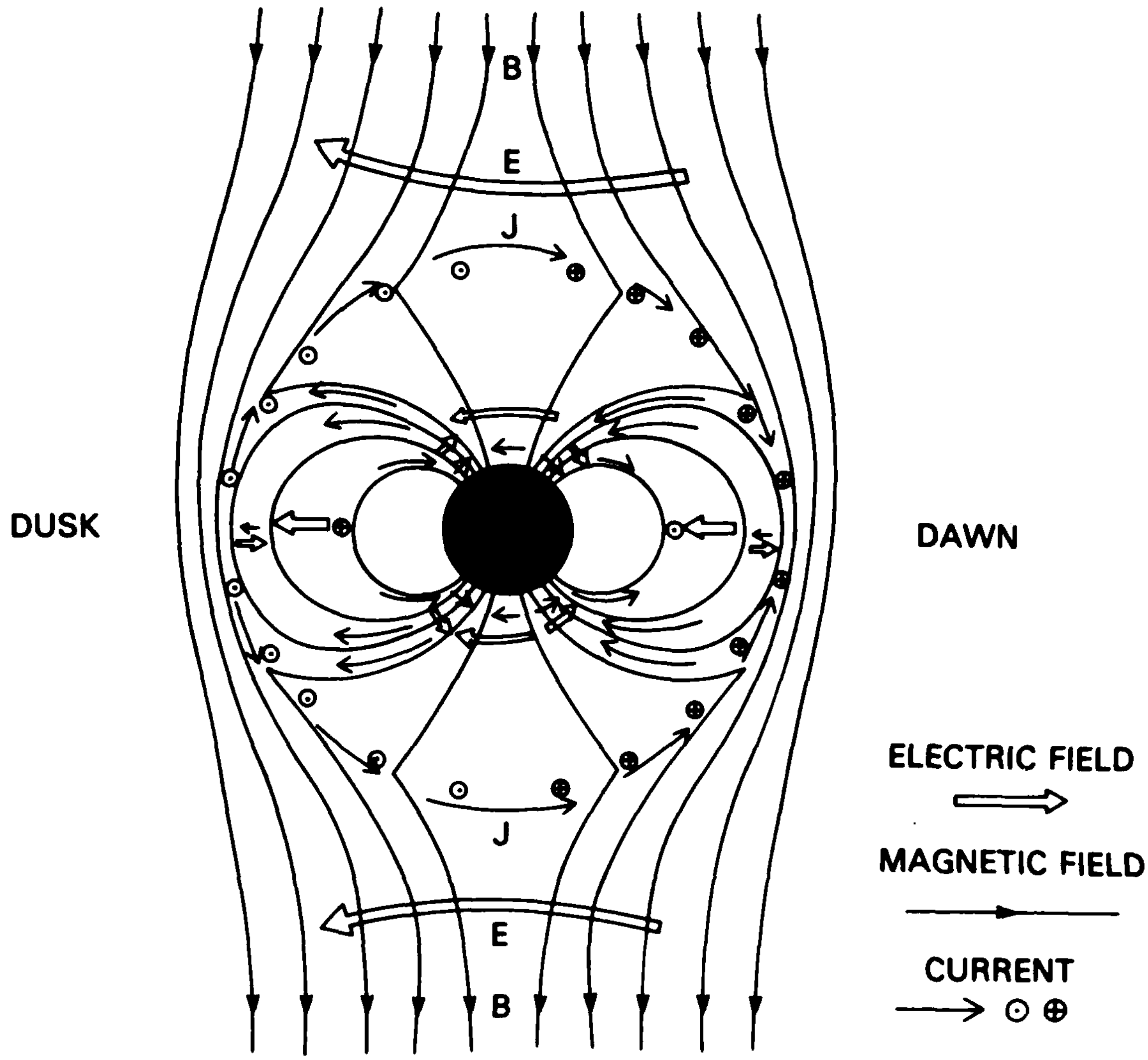

Figure 3. A sketch of the high latitude magnetic field lines, currents, and electric fields observed in the simulation results projected onto a solar-magnetospheric y-z coordinate plane and viewed looking sunward. The Region 1 currents are centered on the last closed field line and connect to the magnetopause where they flow tailward (sunward) at dusk (dawn) before closing perpendicular to the field through the polar dynamo region in the magnetopause-magnetosheath. The Region 2 currents are at lower latitudes closing through the magnetospheric equatorial region sunward (tailward) at dusk (dawn) and duskward through the near-earth plasma sheet. The primary dynamo is on open polar field lines for southward IMF, but there is also a secondary dynamo in the low latitude boundary layer for the Region 1 current on closed field lines which is in series with the polar dynamo.

Distribution List

Director
Naval Research Laboratory
Washington, DC 20375
ATTN: Code 4700 (26 Copies)
Code 4701
Code 4780 (50 copies)
Code 4706 (P. Rodriguez)

Office of Naval Research
Washington, DC 22170
ATTN: Dr. C. Roberson
(Code 412)

Director
Defense Nuclear Agency
Washington, DC 20305
ATTN: Dr. Leon Wittwer
Dr. P. Crowley

Commanding Officer
Office of Naval Research Western
Regional Office
1030 East Green Street
Pasadena, CA 91106
ATTN: R. Brandt

NASA Headquarters
Code EE-8
Washington, DC 20546
ATTN: Dr. S. Shawhan
Dr. D. Butler

NASA/Goddard Space Flight Center
Greenbelt, MD 20771
ATTN: M. Goldstein, Code 692
Robert F. Benson, Code 692
T. Northrop, Code 665
T. Birmingham, Code 695.1
A. Figuero Vinas, Code 692
Shing F. Fung, Code 696
D.S. Spicer, Code 682

Aerospace Corp.
A6/2451, P.O. Box 92957
Los Angeles, CA 90009
ATTN: A. Newman
D. Gorney
M. Schulz
J. Fennel

Bell Laboratories
Murray Hill, NJ 07974
ATTN: A. Hasegawa
L. Lanzerotti

Lawrence Livermore Laboratory
University of California
Livermore, CA 94551
ATTN: Library
B. Kruer
J. DeGroot
B. Langdon
R. Briggs
D. Pearlstein

Los Alamos National Laboratory
P.O. Box 1663
Los Alamos, NM 87545
ATTN: Library
S.P. Gary
N. Quest
J. Brackbill
J. Birn
J. Borovsky
D. Forslund
J. Kindel
B. Bezzerides
C. Nielson
E. Lindman
L. Thode
D. Winske

Lockheed Research Laboratory
Palo Alto, CA 94304
ATTN: M. Walt
J. Cladis
Y. Chiu
R. Sharp
E. Shelley

National Science Foundation
Atmospheric Research Section (ST)
Washington, DC 20550
ATTN: D. Peacock

Physics International Co.
2400 Merced Street
San Leandro, CA 94577
ATTN: J. Benford
S. Putnam
S. Stalings
T. Young

Sandia Laboratories
Albuquerque, NM 87115
ATTN: A. Toepfer
D. VanDevender
J. Freeman
T. Wright

Science Applications, Inc.
Lab. of Applied Plasma Studeis
P.O. Box 2351
LaJolla, CA 92037
ATTN: L. Linson

TRW Space and Technology Group
Space Science Dept.
Building R-1, Room 1170
One Space Park
Redondo Beach, CA 90278
ATTN: R. Fredericks
W.L. Taylor

University of Alaska
Geophysical Institute
Fairbanks, AK 99701
ATTN: Library
S. Akasofu
J. Kan
J. Roederer
L. Lee
D. Swift

University of Arizona
Dept. of Planetary Sciences
Tucson, AZ 85721
ATTN: J.R. Jokipii

Boston College
Department of Physics
Chestnut Hill, MA 02167
ATTN: R.L. Carovillano
P. Bakshi

University of California, S.D.
LaJolla, CA 92037
(Physics Dept.):
ATTN: T. O'Neil
J. Winfrey
Library
J. Malmberg
(Dept. of Applied Sciences):
ATTN: H. Booker

University of California
Space Science Lab
Berkeley, CA 94720
ATTN: M. Temerin
F. Mozer

University of California
Physics Department
Irvine, CA 92664
ATTN: Library
G. Benford
N. Rostoker
C. Robertson
N. Rynn

University of California
Los Angeles, CA 90024
(Physic Dept.):
ATTN: J.M. Dawson
B. Fried
J. Maggs
J.G. Moralles
W. Gekelman
R. Stenzel
Y. Lee
A. Wong
F. Chen
M. Ashour-Abdalla
Library
J.M. Cornwall
R. Walker
P. Pritchett

(Institute of Geophysics and
Planetary Physics):
ATTN: Library
C. Kennel
F. Coroniti

University of Chicago
Enrico Fermi Institute
Chicago, IL 60637
ATTN: E.N. Parker
I. Lerche
Library

University of Colorado
Dept. of Astro-Geophysics
Boulder, CO 80302
ATTN: M. Goldman
Library

Cornell University
School of Applied and Engineering Physics
College of Engineering
Ithaca, NY 14853
ATTN: Library
R. Sudan
B. Kusse
H. Fleischmann
C. Wharton
F. Morse
R. Lovelace
P.M. Kintner

Harvard University
Center for Astrophysics
60 Garden Street
Cambridge, MA 02138
ATTN: G.B. Field
R. Rosner
K. Tsinganos
G.S. Vaiana

University of Iowa
Iowa City, IA 52240
ATTN: C.K. Goertz
D. Gurnett
G. Knorr
D. Nicholson
C. Grabbe
L.A. Frank
K. Nishikawa
N. D'Angelo
R. Merlino
C. Huang

University of Maryland
Physics Dept.
College Park, MD 20742
ATTN: K. Papadopoulos
H. Rowland
C. Wu

University of Maryland, IPST
College Park, MD 20742
ATTN: David Matthews

University of Michigan
Ann Arbor, MI 48140
ATTN: E. Fontheim

University of Minnesota
School of Physics
Minneapolis, MN 55455
ATTN: Library
Dr. J.R. Winckler
Dr. P. Kellogg
Dr. R. Lysak

M.I.T.
Cambridge, MA 02139
ATTN: Library
(Physics Dept.):
ATTN: B. Coppi
V. George
G. Bekefi
T. Chang
T. Dupree
R. Davidson
(Elect. Engineering Dept.):
ATTN: R. Parker
A. Bers
L. Smullin
(R.L.E.):
ATTN: Library
(Space Science):
ATTN: Reading Room

University of New Hampshire
Department of Physics
Durham, NH 03824
ATTN: R.L. Kaufmann
J. Hollweg

Princeton University
Princeton, NJ 08540
Attn: Physics Library
Plasma Physics Lab. Library
F. Perkins
T.K. Chu
H. Okuda
H. Hendel
R. White
R. Kurlsrud
H. Furth
S. Yoshikawa
P. Rutherford

Rice University
Houston, TX 77001
Attn: Space Science Library
T. Hill
R. Wolf
P. Reiff
G.-H. Voigt

University of Rochester
Rochester, NY 14627
ATTN: A. Simon

Stanford University
Radio Science Lab
Stanford, CA 94305
ATTN: R. Helliwell

Stevens Institute of Technology
Hoboken, NJ 07030
ATTN: B. Rosen
G. Schmidt
M. Seidl

University of Texas
Austin, TX 78712
ATTN: W. Drummond
V. Wong
D. Ross
W. Horton

University of Texas
Center for Space Sciences
P.O. Box 688
Richardson, TX 75080
ATTN: David Klumpar

Thayer School of Engineering
Dartmouth College
Hanover, NH 03755
ATTN: Bengt U.O. Sonnerup
M. Hudson

Utah State University
Dept. of Physics
Logan, UT 84322
ATTN: Robert W. Schunk

University of Thessaloniki
Department of Physics
GR-54006 Thessaloniki,
GREECE
ATTN: Dr. L. Vlahos

IONOSPHERIC MODELING DISTRIBUTION LIST
(UNCLASSIFIED ONLY)

PLEASE DISTRIBUTE ONE COPY TO EACH OF THE FOLLOWING PEOPLE (UNLESS OTHERWISE NOTED)

NAVAL RESEARCH LABORATORY
WASHINGTON, DC 20375
- DR. H. GURSKY - CODE 4100
- DR. J.M. GOODMAN - CODE 4180
- DR. P. RODRIQUEZ - CODE 4750
- DR. P. MANGE - CODE 4101
- DR. R. MEIER - CODE 4140
- CODE 2628 (22 COPIES)
- CODE 1220

A.F. GEOPHYSICS LABORATORY
L.G. HANSCOM FIELD
BEDFORD, MA 01731
- DR. T. ELKINS
- DR. W. SWIDER
- MRS. R. SAGALYN
- DR. J.M. FORBES
- DR. T.J. KENESHEA
- DR. W. BURKE
- DR. H. CARLSON
- DR. J. JASPERSE
- DR. F.J. RICH
- DR. N. MAYNARD
- DR. D.N. ANDERSON
- DR. S. BASU

BOSTON UNIVERSITY
DEPARTMENT OF ASTRONOMY
BOSTON, MA 02215
- DR. J. AARONS
- DR. M. MENDILLO

CORNELL UNIVERSITY
ITHACA, NY 14850
- DR. B. FEJER
- DR. R. SUDAN
- DR. D. FARLEY
- DR. M. KELLEY

INSTITUTE FOR DEFENSE ANALYSIS
1801 N. BEAUREGARD STREET
ARLINGTON, VA 22311
- DR. E. BAUER

MASSACHUSETTS INSTITUTE OF TECHNOLOGY
PLASMA FUSION CENTER
CAMBRIDGE, MA 02139
- LIBRARY, NW16-262
- DR. T. CHANG
- DR. R. LINDZEN

NASA
GODDARD SPACE FLIGHT CENTER
GREENBELT, MD 20771
- DR. N. MAYNARD (CODE 696)
- DR. R.F. BENSON
- DR. K. MAEDA
- DR. S. CURTIS
- DR. M. DUBIN

COMMANDER
NAVAL OCEAN SYSTEMS CENTER
SAN DIEGO, CA 92152
- MR. R. ROSE - CODE 5321

NOAA
DIRECTOR OF SPACE AND
ENVIRONMENTAL LABORATORY
BOULDER, CO 80302
- DR. A. GLENN JEAN
- DR. G.W. ADAMS
- DR. K. DAVIES
- DR. R.F. DONNELLY

OFFICE OF NAVAL RESEARCH
800 NORTH QUINCY STREET
ARLINGTON, VA 22217
- DR. G. JOINER

LABORATORY FOR PLASMA AND
FUSION ENERGIES STUDIES
UNIVERSITY OF MARYLAND
COLLEGE PARK, MD 20742
- JHAN VARYAN HELLMAN,
  REFERENCE LIBRARIAN

PENNSYLVANIA STATE UNIVERSITY
UNIVERSITY PARK, PA 16802
DR. J.S. NISBET
DR. P.R. ROHRBAUGH
DR. L.A. CARPENTER
DR. M. LEE
DR. R. DIVANY
DR. P. BENNETT
DR. E. BLEVANS

PRINCETON UNIVERSITY
PLASMA PHYSICS LABORATORY
PRINCETON, NJ 08540
DR. F. PERKINS

SAIC
1150 PROSPECT PLAZA
LA JOLLA, CA 92037
DR. D.A. HAMLIN
DR. L. LINSON
DR. E. FRIEMAN

SRI INTERNATIONAL
333 RAVENSWOOD AVENUE
MENLO PARK, CA 94025
DR. R. TSUNODA
DR. WALTER CHESNUT
DR. CHARLES RINO
DR. J. VICKREY
DR. R. LIVINGSTON

STANFORD UNIVERSITY
STANFORD, CA 94305
DR. P.M. BANKS
DR. R. HELLIWELL

U.S. ARMY ABERDEEN RESEARCH
AND DEVELOPMENT CENTER
BALLISTIC RESEARCH LABORATORY
ABERDEEN, MD
DR. J. HEIMERL

GEOPHYSICAL INSTITUTE
UNIVERSITY OF ALASKA
FAIRBANKS, AL 99701
DR. L.C. LEE

UTAH STATE UNIVERSITY
4TH AND 8TH STREETS
LOGAN, UT 84322
DR. R. HARRIS
DR. K. BAKER
DR. R. SCHUNK
DR. J. ST.-MAURICE
DR. N. SINGH

UNIVERSITY OF CALIFORNIA
LOS ALAMOS NATIONAL LABORATORY
EES DIVISION
LOS ALAMOS, NM 87545
DR. M. PONGRATZ, ESS-DOT
DR. D. SIMONS, ESS-7, MS-D466
DR. L. DUNCAN, ESS-7, MS-D466
DR. P. BERNHARDT, ESS-7, MS-D466
DR. S.P. GARY, ESS-8
DENNIS RIGGIN, ATMOS SCI GRP

UNIVERSITY OF ILLINOIS
DEPARTMENT OF ELECTRICAL ENGINEERING
1406 W. GREEN STREET
URBANA, IL 61801
DR. ERHAN KUDEKI

UNIVERSITY OF CALIFORNIA,
LOS ANGELES
405 HILLGARD AVENUE
LOS ANGELES, CA 90024
DR. F.V. CORONITI
DR. C. KENNEL
DR. A.Y. WONG

UNIVERSITY OF MARYLAND
COLLEGE PARK, MD 20740
DR. K. PAPADOPOULOS
DR. E. OTT

JOHNS HOPKINS UNIVERSITY
APPLIED PHYSICS LABORATORY
JOHNS HOPKINS ROAD
LAUREL, MD 20810
DR. R. GREENWALD
DR. C. MENG
DR. T. POTEMRA

UNIVERSITY OF PITTSBURGH
PITTSBURGH, PA 15213
DR. N. ZABUSKY
DR. M. BIONDI
DR. E. OVERMAN

UNIVERSITY OF TEXAS AT DALLAS
CENTER FOR SPACE SCIENCES
P.O. BOX 688
RICHARDSON, TX 75080
DR. R. HEELIS
DR. W. HANSON
DR. J.P. McCLURE

DIRECTOR OF RESEARCH
U.S. NAVAL ACADEMY
ANNAPOLIS, MD 21402

END
9-87
DTIC